Catalysis Communications 152 (2021) 106286

Contents lists available at ScienceDirect

Catalysis Communications

journal homepage: www.elsevier.com/locate/catcom

Short communication

Verification of impurity-related photocatalytic activity of insulating oxide supports

Bianca Kortewille [a,b], Armin Springer [c], Jennifer Strunk [b,*]

[a] Laboratory of Industrial Chemistry, Ruhr-University Bochum, 44780 Bochum, Germany
[b] Leibniz Institute for Catalysis at the University of Rostock, 18059 Rostock, Germany
[c] Medical Biology and Electron Microscopy Center, Rostock University Medical Center, Strempelstrasse 14, 18057 Rostock, Germany

ARTICLE INFO

Keywords:
Photocatalysis
Selective oxidation
Methanol
DRIFTS
Active site

ABSTRACT

Photocatalysts composed of vanadium oxide species supported on commercial MgO and ZrO_2 are investigated in selective methanol oxidation. Both support oxides are insulators, so the vanadium oxide species are expected as sole active component in photocatalysis. However, the pure supports showed considerable activity: Bare MgO was more active than MgO-supported vanadia catalysts, and ZrO_2 showed intermediate activity. By various characterization methods, the presence of TiO_2 (anatase) in the MgO support, and the presence of Zn, possibly as ZnO, in ZrO_2 is demonstrated. The present study highlights that photocatalysts containing commercial supports must be carefully checked for impurity-related photocatalytic performance.

1. Introduction

In heterogeneous catalysis, identification of active sites is a prerequisite for a knowledge-based improvement of catalysts. In thermal catalysis, extensive characterization of catalysts occasionally allowed identifying nature and location of the active site, for instance, for vanadium oxide-based catalysts for selective oxidation reactions [1]. In photocatalysis, on the other hand, a methodology for reliable studies of active sites, ideally in operando, still needs to be established.

In previous studies [2,3], we demonstrated the applicability of isolated and oligomerized vanadium oxide (VO_x) species as photocatalysts for selective oxidation of methanol. These results provided an example for the transfer of a known active site from classical catalysis [4–7] to the field of photocatalysis. Isolated VO_4 sites were demonstrated to be beneficial in terms of activity and selectivity compared to oligomers, and V_2O_5 crystallites were inactive for photocatalytic methanol oxidation. For silica and alumina as supports, the absence of any activity (silica) or at least only negligible activity (alumina) was proven [2,3]. Tests of a multitude of supports are desirable, since the nature of the support influences the structure of the VO_x species. Furthermore, for isolated VO_4 species in thermal catalytic methanol oxidation the turnover frequencies depend on the electronegativity of the support cation and may additionally be correlated with the reducibility of the oxide support [5–8]. Magnesium and zirconium oxide appear as suitable candidates, as they strongly differ in their points of zero charge (MgO: 11; ZrO_2: ~6) [9] and possess wide band gaps (MgO: 7.8 eV, ZrO_2: 5.2 eV) [10,11]. Since in photocatalysis under ambient conditions the presence of water cannot be avoided, the structure of the VO_x species under moist conditions must be expected. So, VO_x species present on MgO are expected to be mainly isolated, while those on ZrO_2 are expected to be oligomerized [12].

In several previous catalytic studies [13–16] decisive influences of additives and impurities have been shown. For example, carbon residues on the catalyst surface were found to be involved in surface reactions during photocatalytic CO_2 reduction [13,14]. In thermal catalyzed oxidative dehydrogenation of propane and ethane by supported vanadia catalysts, additives like main group elements (P, K) and transition metal ions (Ni, Cr, Nb, Mo) were found to modify the catalyst's acid-base properties and reducibility, and consequently their selectivity and activity [15,16].

Initially, the goal of this study was to characterize the structure and electronic properties of magnesia- and zirconia-supported VO_x catalysts, and to correlate these properties with their catalytic activity. However, the pure supports showed an apparent high activity without any vanadium oxide deposition. We demonstrate that photocatalysts containing commercial support materials must be carefully checked for impurities which potentially affect or even dominate photocatalytic performance.

* Corresponding author.
E-mail address: jennifer.strunk@catalysis.de (J. Strunk).

https://doi.org/10.1016/j.catcom.2021.106286
Received 10 December 2020; Received in revised form 22 January 2021; Accepted 27 January 2021
Available online 2 February 2021

2. Experimental

Commercial MgO (nanopowder, 99.5%, STREM) and ZrO_2 (monoclinic, 99% metals basis excluding Hf, Alfa Aesar) were used as support materials. Both supports have a very high purity as indicated by the supplier. VO_x was deposited *via* impregnation with ammonium metavanadate (AMV). The synthesis procedure is described in detail in Ref. [3]. Exact synthesis parameters are summarized in Table S1 in the Supplementary Information (SI). Catalysts are labeled as V(x)/Support, according to their vanadium loading x in V per nm^2.

The vanadium content was determined by atomic absorption spectroscopy (AAS) using an AAS 6 vario (Analytik Jena). Portable energy dispersive X-ray fluorescence spectroscopy (pXRF) using a Niton Xl3t GOLDD instrument was carried out to analyze the composition of the catalysts. ICP-MS (Element XR, ThermoScientific) was performed for V(1.2)/MgO to determine the exact Ti content. Specific surface areas were determined by N_2 physisorption (Bellsorp max; Belcat, Inc.) using the BET method. The structure and electronic properties of the catalysts were analyzed by Raman and UV–vis diffuse reflectance spectroscopy (UV–Vis DRS) corresponding to the procedures described previously [2,3]. Raman spectroscopy was performed under ambient conditions. MgO-supported samples were measured with a 442 nm laser, to avoid fluorescence caused by the 532 nm laser. In UV–Vis DRS, catalyst spectra were collected using $BaSO_4$ as white standard. Powder X-ray diffraction (PXRD) was measured in a 2θ range from 5 to 80° (Malvern Panalytical Empyrean diffractometer, CuKα radiation, λ = 1.54 Å).

Photocatalytic methanol oxidation was studied *in situ* by diffuse reflectance infrared Fourier transform spectroscopy (DRIFTS). For information on the spectrometer, *in situ* cell, and sample pretreatment, please refer to the SI. Methanol was fed to the sample in the IR cell at ~35 to 38 °C by passing a nitrogen flow (20 ml min^{-1}) through a saturator maintained at 0 °C using an ice bath. After 10 min of methanol adsorption, the gas flow was switched back to synthetic air (20 ml min^{-1}) and the IR cell was purged for at least 10 min. Subsequently, irradiation of the catalyst was started *via* focusing the light of a 150 W Xe lamp onto the catalyst inside the spectrometer through an optical fiber. IR radiation was cut off using an optical IR filter, transmitting in the range of 320 to 760 nm. During irradiation, spectra were acquired as

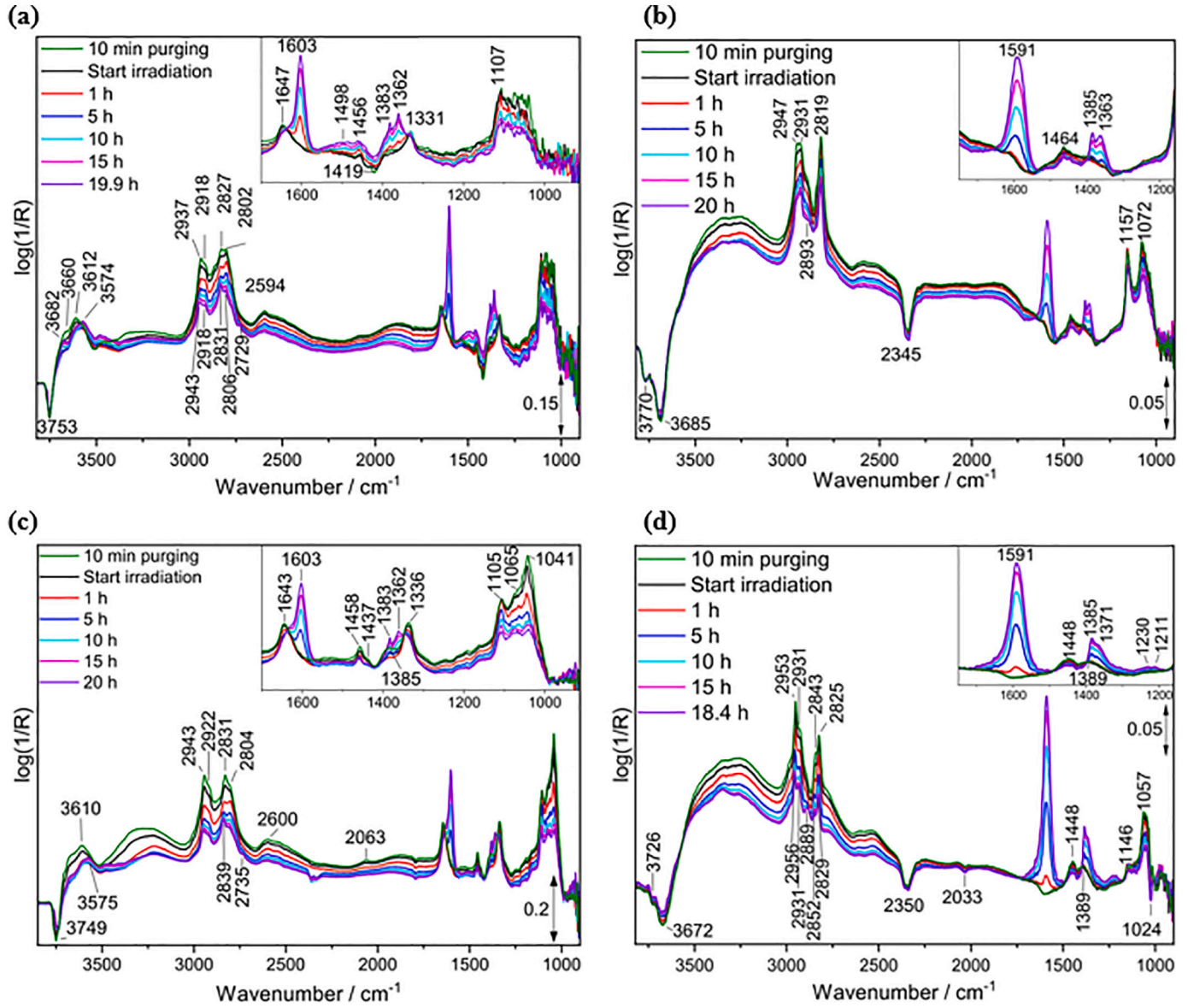

Fig. 1. *In situ* DRIFT difference spectra of (a) MgO, (b) ZrO_2, (c) V(1.2)/MgO, (d) V(2.6)/ZrO_2 during photocatalytic oxidation of adsorbed methanol; inset displays zoom of the region between 1700 and 900 cm^{-1}. (For interpretation of the references to colour in this figure legend, the reader is referred to the web version of this article.)

series. All spectra are displayed as difference spectra, referenced to the spectrum of the pretreated catalyst.

3. Results and discussion

As reported in previous studies [17,18] and demonstrated for related alumina- and silica-supported catalysts [2,3], vanadium oxide (VO_x) catalysts with loadings ranging from 1.2 to 12.7 V atoms per nm^2 can be synthesized reproducibly by impregnation. VO_x loading on the ZrO_2 support hardly affects the specific surface area (~15 $m^2\ g^{-1}$). However, the surface area of the calcined MgO support (62 $m^2\ g^{-1}$) is slightly increased upon impregnation with aqueous AMV (~68 to 69 $m^2\ g^{-1}$), possibly due to hydration of the MgO surface layers and the resulting modification in the morphology of the MgO microcrystals [19]. Mixed magnesia-vanadia phases may be produced, possibly with part of the vanadium centers covered by MgO layers [20]. More information on sample characterization can be found in the SI (Table S2). UV–Vis spectroscopy (see SI) already indicates the presence of impurities absorbing in the UV–Vis range, because ZrO_2 shows a tailing from its absorption edge at ~5 eV [10,21] down to ~3.2 eV (387 nm), which corresponds to the band gap of ZnO [22]. For MgO, pronounced absorption down to 3.5 eV is observed, which may indicate the presence of TiO_2 [21] affected by the quantum size effect [23].

In Fig. 1 the difference spectra of the pure MgO and ZrO_2 supports (Fig. 1a and b), the V(1.2)/MgO (Fig. 1c) and the V(2.6)ZrO_2 sample (Fig. 1d) during photocatalytic oxidation of adsorbed methanol are displayed. Measurements of the samples with higher loading and reference experiments without illumination ("dark experiments") are shown in Figs. S4 and S5. Only bands directly related to methanol oxidation will be discussed here. For a more detailed discussion, please see the SI.

Essentially the same bands appear for all samples, but relative intensities differ. Methanol adsorption causes negative bands at ~3750 cm^{-1} for MgO-based samples, and at ~3770 and ~3680 cm^{-1} for ZrO_2-based samples, indicating the perturbation of isolated surface hydroxyls on the support surface [24,25]. Related negative bands appear in all V/MgO samples, which indicates that free MgO surface hydroxyls are still exposed, despite high VO_x loading. It implies that mixed V-Mg oxides have been formed rather than a full surface monolayer of VO_x.

On ZrO_2 the gradual disappearance of the negative bands at increasing VO_x surface coverage indicates formation of a partial surface monolayer in V(2.6)/ZrO_2, whereas monolayer coverage is exceeded in V(12.7)/ZrO_2. Several broad positive bands between 3610 and ~3100 cm^{-1} are formed on MgO-based samples, caused by an increase in the number of interacting hydroxyl groups due to the presence and dissociation of adsorbed methanol [26].

Vibrations of vanadia-bound methoxy species occur at 2930 and 2830 cm^{-1} [26,27], and methoxy species bound to ZrO_2 display bands at 2931 and 2819 cm^{-1} [28,29]. The shoulder at 2947 cm^{-1} is most likely assignable to a second differently coordinated methoxy species. The complex pattern for the MgO-supported catalysts cannot be fully unraveled, but clearly methanol binds to the surface. Bands at 1107, 1065, and 1045 cm^{-1} for pure MgO and the MgO-supported catalysts are assigned to ν(C—O) of monodentate and bridged methoxy species as well as to molecularly adsorbed methanol, respectively [28,30–32]. The ν(C—O) band at 1045 cm^{-1} and the broad band of interacting OH groups significantly decrease in intensity during the first hour of the reaction, irrespective of sample irradiation, indicative of a weakly bound, undissociated methanol species. On ZrO_2, two bands at 1157 and 1072 cm^{-1} associated with ν(C—O) support the presence of two chemisorbed methoxy species [28,29] after methanol adsorption.

Upon irradiation, bands appear at 1603, 1383 and 1362 cm^{-1} for the MgO-based samples, and at 1591, 1385 and ~1370 cm^{-1} for the ZrO_2-based samples. These bands are assigned to formate species bound to either the support or the VO_x species. For the MgO-supported samples, relative to the height of the bands of adsorbed methanol, the formate bands are strongest on the bare support, and the intensity decreases with increasing VO_x loading. For the ZrO_2-based samples, the intensity of the formate bands relative to the bands of adsorbed methanol follow the order V(2.6)/ZrO_2 > ZrO_2 > V(12.7)/ZrO_2. Please note that DRIFTS is not a quantitative technique, so the comparison of relative band heights can only yield a rough estimate on the relative amount of surface adsorbate. No formate formation is observed in dark experiments. For discussion of the bands at ~1643, 1456, and 1340 cm^{-1}, remaining unchanged during irradiation, please see SI.

The results demonstrate that methanol is photocatalytically oxidized to formate on all samples. Both seemingly "bare" insulating supports can carry out this light-induced reaction. Moreover, the activity of the MgO support is higher than that of the corresponding VO_x catalysts. The ZrO_2 support shows an activity in between the two VO_x-loaded samples.

The semiquantitative analysis by pXRF reveals several impurities in the commercial oxide supports and in the corresponding supported VO_x catalysts. Considering all impurities with >0.1 wt%, a contamination of the ZrO_2 with ~0.5 wt% Zn, ~0.3 wt% Cu, and ~0.2 wt% S was detected. In MgO, ~0.6 wt% Ti, ~0.4 wt% Fe, ~0.1 wt% Mn, ~0.8 to 1.4 wt% Ca, and ~0.1 to 0.4 wt% Cl were found. For an overview over all samples, please see the SI, Tables S3 and S4. Since almost identical amounts of impurities are detected in the oxide supports and the corresponding VO_x catalysts, it is concluded that they originate from the oxide support, and contamination did not occur during synthesis. The contaminants with the highest concentrations were Zn in case of ZrO_2 and Ti in case of MgO. Their corresponding oxides, TiO_2 (especially in the anatase phase) and ZnO, are semiconductors exhibiting band gaps of ~3.2 eV [21,22], well-known as active photocatalysts for a multitude of reactions.

In addition to pXRF, the Ti content of V(1.2)/MgO was analyzed exemplary by ICP-MS. The resulting titanium content of 0.14 wt% is approximately four times lower than determined by pXRF, because the error of pXRF may be relatively high. A systematic error seems likely, since reproducible and comparable titanium contents were obtained for all magnesia samples.

Crystalline phases were identified by Raman spectroscopy (Fig. 2) for the MgO-based samples. Although the spectrum of the MgO support is expected to be essentially featureless in the depicted region, Raman bands at 140, 196, 206, 393, 513, 638, and 1094 cm^{-1} are observed. The latter has previously been assigned to carbonate species present on MgO [15]. All other bands are unambiguously attributed to vibrational modes of anatase phase TiO_2 by comparison with reference spectra (RRUFF database; RRUFF ID = R120013 and R070582). This is additionally supported by XRD results (Fig. S6). The anatase bands are still present in the MgO-supported catalysts. However, with increased vanadia loading their intensity decreases, likely due to the presence of VO_x species, which are also Raman active. Isolated VO_4 species are identified in the low-loaded sample by their characteristic band at ~820 cm^{-1}. In addition, magnesium ortho- and -pyrovanadates are found in the highly loaded sample.

The Raman spectrum of ZrO_2 and the ZrO_2-supported VO_x catalysts (Fig. S7) displays various bands assigned to the support, to oligomerized VO_x species, and V_2O_5 nanoparticles. It shows various additional bands (809, 852, 905, 988, and 1014 cm^{-1}), likely assignable to impurities. However, a comparison with the respective entries from the RRUFF database shows that they do not originate from ZnO, ZnS, CuO, Cu_2O, $Cu_2V_2O_7$, or different hydrates of $ZnSO_4$ and $CuSO_4$. Possibly, the structures formed from the impurities are too small, or their concentration is too low, to detect them. Since the amount of sulfur in the ZrO_2 seems considerably lower than the amount of Zn, we suggest that the primary photoactive component is ZnO. This is supported by the UV–Vis spectra, which show an absorption corresponding to ZnO (3.2 eV) [22], but not matching the band gaps of ZnS (~3.7 eV) [33], CuO (1.2 to 1.75 eV) [34,35], or Cu_2O (~2.0 to 2.1 eV) [34].

Scanning electron microscopy of the MgO support confirms the presence and inhomogeneous distribution of Ti in the flake-structured

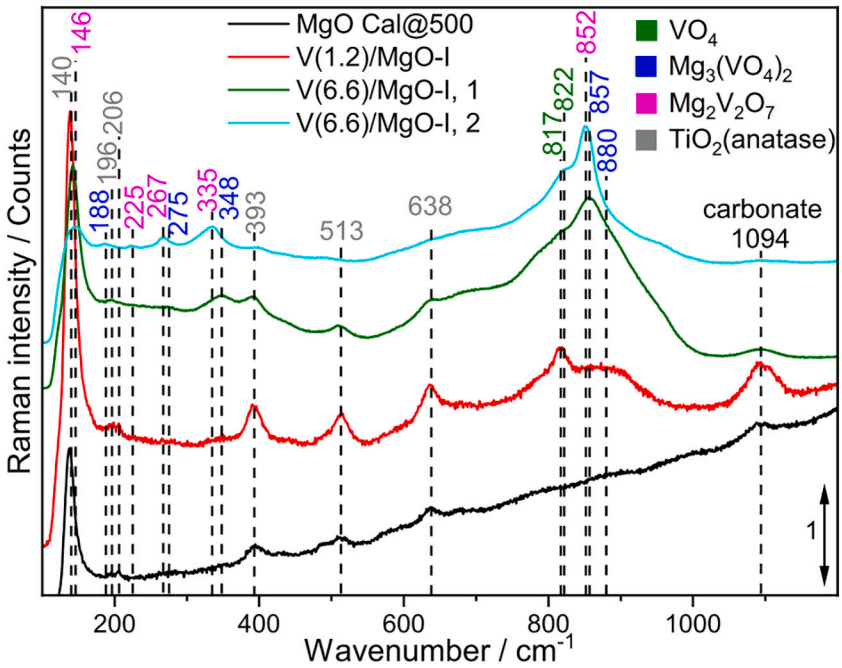

Fig. 2. Raman spectra of MgO-supported catalysts in comparison to the pure MgO support, taken under ambient conditions using the blue laser (442 nm); spectra were normalized to the band at 394 nm and averaged over four spectra. (For interpretation of the references to colour in this figure legend, the reader is referred to the web version of this article.)

oxide (Fig. S8, Fig. S9). For the ZrO_2 support (Fig. 3, Fig. S10) the presence of Zn is confirmed, too. Zn is much more homogeneously distributed, although it also concentrates in certain regions. Still, the concentration might be too low to form crystalline structures. EDX analysis of larger sample regions confirms the impurity concentrations detected by means of pXRF and ICP-MS, because 0.18 ± 0.03 wt% Ti are detected in MgO, whereas 0.44 ± 0.05 wt% Zn was found in ZrO_2.

The relative photocatalytic activity of the samples can then be rationalized as follows: In the commercial MgO, anatase impurities are exposed at the surface, which cause the photocatalytic oxidation of methanol to formate. Upon VO_x deposition, isolated VO_x and magnesia-vanadia mixed phases are formed, which partially cover up the exposed titania. Since the photocatalytic activity of those newly formed phases under the applied illumination (320 to 760 nm) is lower than that of anatase, the photocatalytic activity decreases with increased vanadia loading. For ZrO_2, ZnO exposed at the surface similarly causes the observed photocatalytic activity. In this case, the activity of the deposited VO_x species either exceeds that of the exposed ZnO, or the ZnO is not covered by the vanadium oxide species, so that both moieties contribute to the photocatalytic activity in V(2.6)/ZrO_2. When monolayer coverage is exceeded in V(12.7)/ZrO_2, both the ZnO is covered, and photocatalytically inactive V_2O_5 is predominantly formed, so this sample is least active.

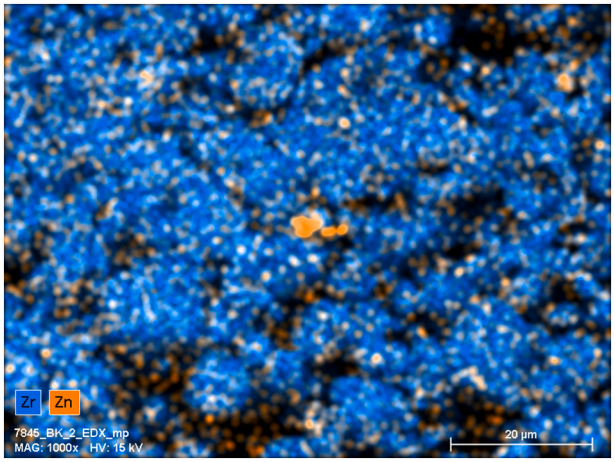

Fig. 3. Elemental mapping of the pure ZrO_2 support.

4. Conclusions

While attempting to study the photocatalytic activity of vanadium oxide species supported on two exemplary highly pure MgO- and ZrO_2-supports in selective methanol oxidation, an unexpected activity of the bare supports was observed. Since the pure supports are supposed to be insulators, impurities are suggested to be responsible for this observation. For the MgO support, the presence of <1 wt% Ti was detected. The amount is sufficient to detect anatase phase TiO_2 by XRD and Raman spectroscopy. This also explains the absorption onset of the MgO support at ~3.5 eV, and it indicates that the TiO_2 moieties are probably small enough to be affected by the quantum size effect. Small amounts of zinc are found in the ZrO_2 support. Although less clearly identifiable, the absorption at ~3.2 eV indicates that ZnO may be present. Both TiO_2 and ZnO are known as highly active photocatalysts for numerous reactions. It cannot be clarified where exactly the impurities originate from, but it is assumed that they may originate from natural ores and/or industrial grade starting materials. The study highlights the importance to conduct blank experiments with pure commercial support materials, because they may contain small amounts of impurities with large photocatalytic activity, so the effect of other deliberately introduced photocatalyst components may be severely overestimated.

Author contributions

B. K. performed all sample syntheses, sample characterization (unless otherwise noted in the acknowledgements), all photocatalytic experiments, and processed the data. A.S. performed the detailed characterization by means of electron microscopy. J.S. designed the study and provided ideas and guidance. All authors critically discussed the data in the context of literature and wrote the manuscript together.

Declaration of Competing Interest

The authors declare that they have no known competing financial interests or personal relationships that could have appeared to influence the work reported in this paper.

Acknowledgements

Part of this work has been funded by the Mercator Research Center Ruhr, Project Pr-2013-0047 “Photoactive Oxide Materials for the Visible Spectral Range”. A. Diekmann, Deutsches Bergbaumuseum Bochum, is acknowledged for supplying the pXRF and ICP-MS measurements. The authors would like to thank M. Muhler, Ruhr-University Bochum, for fruitful scientific discussions and the opportunity to use scientific equipment (IR spectroscopy, UV–Vis spectroscopy, N_2 physisorption) in his laboratories. Similarly, the authors would like to thank I.E. Wachs, Lehigh University, for fruitful scientific discussions and the chance to measure Raman spectroscopy in his laboratories. G. Bacher and O. Pfingsten, University Duisburg-Essen, are acknowledged for fruitful scientific discussions.

Appendix A. Supplementary data

Supplementary data to this article can be found online at https://doi.org/10.1016/j.catcom.2021.106286.

References

[1] I.E. Wachs, Catal. Today 100 (2005) 79–94.
[2] B. Kortewille, I.E. Wachs, N. Cibura, O. Pfingsten, G. Bacher, M. Muhler, J. Strunk, ChemCatChem 10 (2018) 2360–2364.
[3] B. Kortewille, I.E. Wachs, N. Cibura, O. Pfingsten, G. Bacher, M. Muhler, J. Strunk, Eur. J. Inorg. Chem. (2018) 3725–3735.
[4] G. Busca, A.S. Elmi, P. Forzatti, J. Phys. Chem. 91 (1987) 5263–5269.
[5] W.C. Vining, A. Goodrow, J. Strunk, A.T. Bell, J. Catal. 270 (2010) 163–171.
[6] L.J. Burcham, I.E. Wachs, Catal. Today 49 (1999) 467–484.
[7] G. Deo, I.E. Wachs, J. Catal. 146 (1994) 323–334.
[8] J.L. Bronkema, A.T. Bell, J. Phys. Chem. C 112 (2008) 6404–6412.
[9] I.E. Wachs, Dalton Trans. 42 (2013) 11762–11769.
[10] C. Gionco, M.C. Paganini, E. Giamello, R. Burgess, C. Di Valentin, G. Pacchioni, J. Phys. Chem. Lett. 5 (2014) 447–451.
[11] D.M. Roessler, W.C. Walker, Phys. Rev. 159 (1967) 733–738.
[12] J. Strunk, M.A. Bañares, I.E. Wachs, Top. Catal. 60 (2017) 1577–1617.
[13] C.-C. Yang, Y.-H. Yu, B. van der Linden, J.C.S. Wu, G. Mul, J. Am. Chem. Soc. 132 (2010) 8398–8406.
[14] B.T. Mei, A. Pougin, J. Strunk, J. Catal. 306 (2013) 184–189.
[15] A. Klisinska, S. Loridant, B. Grzybowska, J. Stoch, I. Gressel, Appl. Catal. A: General 309 (2006) 17–27.
[16] A. Klisinska, K. Samson, I. Gressel, B. Grzybowska, Appl. Catal. A: General 309 (2006) 10–16.
[17] T. Machej, J. Haber, A.M. Turek, I.E. Wachs, Appl. Catal. 70 (1991) 115–128.
[18] S.T. Oyama, G.T. Went, K.B. Lewis, A.T. Bell, G.A. Somorjai, J. Phys. Chem. 93 (1989) 6786–6790.
[19] E.F. Aboelfetoh, M. Fechtelkord, R. Pietschnig, J. Mol. Catal. A Chem. 318 (2010) 51–59.
[20] G. Martra, F. Arena, S. Coluccia, F. Frusteri, A. Parmaliana, Catal. Today 63 (2000) 197–207.
[21] Y. Xu, M.A.A. Schoonen, The American Mineralogist 85 (2000) 543–556.
[22] T. Inoue, A. Fujishima, S. Konishi, K. Honda, Nature 277 (1979) 637–638.
[23] M. Anpo, P.V. Kamat, Environmentally Benign Photocatalysts: Applications of Titanium Oxide-based Materials, Springer New York, 2010.
[24] E. Knözinger, K.-H. Jacob, S. Singh, P. Hofmann, Surf. Sci. 290 (1993) 388–402.
[25] C. Chizallet, G. Costentin, M. Che, F. Delbecq, P. Sautet, J. Am. Chem. Soc. 129 (2007) 6442–6452.
[26] G. Busca, Catal. Today 27 (1996) 457–496.
[27] L.J. Burcham, L.E. Briand, I.E. Wachs, Langmuir 17 (2001) 6164–6174.
[28] C. Chizallet, M.L. Bailly, G. Costentin, H. Lauron-Pernot, J.M. Krafft, P. Bazin, J. Saussey, M. Che, Catal. Today 116 (2006) 196–205.
[29] M. Bensitel, V. Moraver, J. Lamotte, O. Saur, J.-C. Lavalley, Spectrochim. Acta A: Mol. Spectrosc. 43 (1987) 1487–1491.
[30] M. Bensitel, O. Saur, J.-C. Lavalley, Mater. Chem. Phys. 28 (1991) 309–320.
[31] F. Khairallah, A. Glisenti, J. Mol. Catal. A Chem. 274 (2007) 137–147.
[32] C. Chizallet, G. Costentin, H. Lauron-Pernot, J.M. Krafft, P. Bazin, J. Saussey, F. Delbecq, P. Sautet, M. Che, Oil & Gas Sci. Technol. - Revue de l’IFP 61 (2006) 479–488.
[33] T.K. Tran, W. Park, W. Tong, M.M. Kyi, B.K. Wagner, C.J. Summers, J. Appl. Phys. 81 (1997) 2803–2809.
[34] M.T.S. Nair, L. Guerrero, O.L. Arenas, P.K. Nair, Appl. Surf. Sci. 150 (1999) 143–151.
[35] Y.K. Jeong, G.M. Choi, J. Phys, Chem. Solids 57 (1996) 81–84.